

Electronic Energy Bands in Strontium Titanate†

A. H. KAHN AND A. J. LEYENDECKER
National Bureau of Standards, Washington, D. C.
 (Received 1 April 1964)

A theoretical examination of the electronic energy bands of cubic strontium titanate has been performed by application of the LCAO (linear combination of atomic orbitals) method. Diagonal energies were determined from ionization potentials and crystalline fields based on a point-charge model for the ions. The ionic charges were adjusted to give agreement with the observed energy gap. Overlap integrals were estimated from free-ion wave functions. For the crystals studied, the calculations led to filled valence bands derived primarily from oxygen $2p$ orbitals and empty conduction bands derived predominantly from titanium $3d$ orbitals. In cubic strontium and barium titanates, there are six lowest-conduction-band ellipsoids lying along $\langle 100 \rangle$ directions of k space with minima probably at the edges of the Brillouin zone. The longitudinal mass is about $20\text{--}50 m_0$ and the transverse mass about $1 m_0$. Spin-orbit splitting removes degeneracy at $k=0$ and leads to additional conduction bands several hundredths of an eV above the lowest conduction band. Comparison is made with experimental data on conductivity, Hall effect, thermoelectric power, reflectivity, and soft x-ray emission. Results are in substantial agreement with experiment.

I. INTRODUCTION

NUMEROUS studies on oxide semiconductors raise questions concerning the electronic band structures in these compounds. In¹ TiO_2 and² SrTiO_3 , at low temperatures, mobilities as large as $10^3 \text{ cm}^2/\text{V}\text{-sec}$ are observed, which decrease with increasing temperatures. This favors a band model for conduction, rather than the hopping picture. It is to be noted that many of the transition metal oxides have in common an ionic coordination consisting of a transition metal ion surrounded by six oxygen ions. As a prototype case for study we have chosen cubic SrTiO_3 because of calculational simplifications arising from its simple cubic structure and the availability of samples for experimentation. Figure 1 shows the unit cell and Brillouin zone for this structure.

The LCAO or tight binding method for treating Bloch functions³ in crystals has been studied carefully by Slater and Koster.⁴ They have found that it is frequently possible to interpolate the results of very

precise calculations (augmented plane-wave method, and others) with LCAO eigenvalues by using only a small number of two-center overlap integrals as disposable parameters. An example of this is given in the augmented plane wave study of NiO by Switendick.⁵ It is expected that this method will be most successful in the case of narrow bands, as, for example, in the transition metal oxides. A critical examination of the method is given by Jones.⁶

It is our suggestion that the LCAO method may be useful for obtaining semiquantitative information about the energy bands in cases too complicated for precise calculation. Wherever possible, we employ empirical data to fix the parameters of the problem. We also note that the results of studies on transition metal ion complexes, such as those of Sugano and Shulman,⁷ give evidence which can be used in estimating parameters in the energy band calculation.

In part II we present simple considerations, based on an ionic model, which indicate which orbitals are significant in considering the energy bands of SrTiO_3 . Parts III and IV contain discussion of the tight binding treatment and the significance of the results.

II. IONIC APPROXIMATION

Perhaps the simplest considerations which give an idea of the energy level structure is the ionic model discussed by Seitz,⁸ which considers the electrons to be in free ionic states shifted by the Madelung potential energies associated with the ionic sites. This has been performed for the perovskite structure. The Madelung potentials were obtained as linear combinations of the

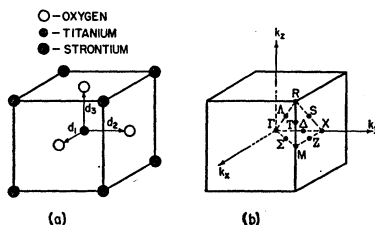


FIG. 1. (a) Unit cell of the perovskite structured strontium titanate. (b) Brillouin zone for the simple cubic crystal, O_h^h . Notation is according to BSW, Ref. 13.

† An abbreviated report on this work has been presented at the 1963 Buhl International Conference on Materials, Pittsburgh, Pennsylvania.

¹ H. P. R. Frederikse, *J. Appl. Phys. Suppl.* **32**, 2211 (1961); J. H. Becker and W. R. Hosler, *J. Phys. Soc. Japan*, **18**, Suppl. II, 152 (1963).

² H. P. R. Frederikse, W. R. Thurber, and W. R. Hosler, *Phys. Rev.* **134**, A442 (1964).

³ F. Bloch, *Z. Physik* **52**, 555 (1928).

⁴ J. C. Slater and G. F. Koster, *Phys. Rev.* **94**, 1498 (1954).

⁵ A. C. Switendick, Quarterly Progress Report No. 49, July 15, 1963, Solid State and Molecular Theory Group, MIT, Cambridge, Massachusetts (unpublished).

⁶ H. Jones, *The Theory of Brillouin Zones and Electronic States in Crystals* (North-Holland Publishing Company, Amsterdam, 1960), pp. 216–229.

⁷ S. Sugano and R. G. Shulman, *Phys. Rev.* **130**, 517 (1963).

⁸ F. Seitz, *The Modern Theory of Solids* (McGraw-Hill Book Company, Inc., New York, 1940), pp. 447–450.

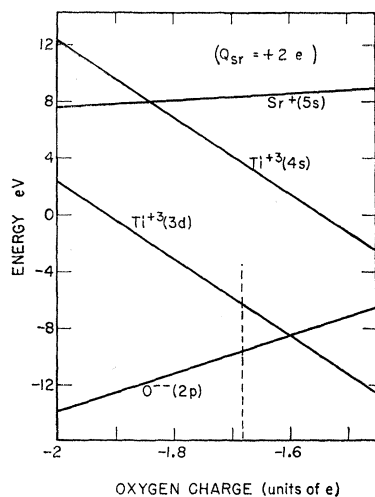


FIG. 2. Plot of energies on the ionic model as a function of oxygen charge. The energy to excite an electron from an oxygen ($2p$) state to various states on cations is represented by the vertical distances from the $O^{--}(2p)$ line.

Madelung constants of the ReO_3 , CsCl , and NaCl structures.⁹ We have made an innovation in allowing the charges of the ions to deviate from the full ionic values in calculating the Madelung potentials. Figure 2 shows a plot of the sum of Madelung and ionization potential energies for an electron at various ionic sites of SrTiO_3 , plotted against oxygen charge. (The Sr charge is held at $2|e|$; the results are very insensitive to the magnitude of the Sr charge.) The separation of filled $2p$ and empty $3d$ levels of ~ 15 eV for full ionicity is typical of many other oxides of transition metals, e.g., BaTiO_3 , TiO_2 , NiO ,¹⁰ and Cu_2O . We attribute the band gap to the $2p$ - $3d$ energy separation and believe that the observed gap of ~ 3 eV indicates a departure from perfect ionicity. We note from Fig. 2 that the $3d$ - $2p$ separation is very sensitive to degree of ionicity. The dotted line of Fig. 2 indicates that an ionicity of 85% is to be expected for an observed gap of 3.25 eV. This value is consistent with the degree of covalency necessary to explain the $\sim 20\,000\text{ cm}^{-1}$ splitting ($10Dq$) of the $3d$ states in Ti-alum¹¹ or Ti in corundum.¹² Also, it is of the order to be expected from estimates of overlap integrals.

This interpretation differs from the approach in which the 15 eV is reduced as a result of division by an appropriate dielectric constant.¹⁰

We note that the Sr- $5s$ level is about 15 eV higher than the Ti- $3d$ level. For this reason we neglect Sr orbitals in the calculation. Also, we drop the Ti- $4s$

and O- $2s$ states, as they are at least 10-eV above or below the $3d$ states. The remoteness of these other states lends credibility to a tight binding treatment which uses $2s$ and $3d$ orbitals only.

III. SYMMETRIZED BLOCH SUMS AND SECULAR EQUATIONS

Cubic SrTiO_3 is of the perovskite structure with the simple cubic space group $O_h^1(Pm3m)$. The unit cell of the perovskite structure is shown in Fig. 1. The irreducible representations of the groups of the wave vector for the space group O_h^1 were first published by Bouckaert, Smoluchowski, and Wigner¹³ (BSW), whose notation we follow. Bloch sums were constructed from titanium $3d$ orbitals based on the centers of the cells. These are of the form, for example,

$$(xy) \equiv (1/N^{1/2}) \sum_i e^{i\mathbf{k}\cdot\mathbf{R}_i} \phi_{xy}(\mathbf{r}-\mathbf{R}_i), \quad (1)$$

where the \mathbf{R}_i run over the primitive cubic lattice sites, ϕ_{xy} is a normalized Ti^{3+} wave function, and \mathbf{k} is the wave vector. The other d states will be appropriately labeled. The p states based on the oxygen sites are made into Bloch sums of the form

$$\frac{1}{\sqrt{2}}(y, -x, 0) = \frac{1}{(2N)^{1/2}} \sum_{i,j} [e^{i\mathbf{k}\cdot(\mathbf{R}_i+\mathbf{d}_1)} \phi_y(\mathbf{r}-\mathbf{R}_i-\mathbf{d}_1) - e^{i\mathbf{k}\cdot(\mathbf{R}_i+\mathbf{d}_2)} \phi_x(\mathbf{r}-\mathbf{R}_i-\mathbf{d}_2)]. \quad (2)$$

In the above, the letters x, y, z signify the three types of normalized p orbitals ϕ_x, ϕ_y, ϕ_z . The three vectors $\mathbf{d}_1, \mathbf{d}_2, \mathbf{d}_3$ give the basis positions of the oxygen ions relative to the titanium at the cell center. The entries in the parentheses give the type of $2p$ orbitals of the three oxygen sites in numerical order, according to Fig. 1.

Table I lists the symmetrized Bloch sums for all lines and points of symmetry in the Brillouin zone (BZ). Strontium s orbitals are all of the identity representation, but are not used.

The energy matrix and secular equations are constructed by taking matrix elements of the Hamiltonian between titanium and oxygen Bloch sums of the same symmetry type only.¹⁴ An actual evaluation of the matrix elements will not be attempted, but rather the values of overlap integrals appropriate to analogous situations in other solids and molecules will be used.

A. Estimates of Matrix Elements

Numerical values of the parameters used for the secular equations are given in Table II.

⁹ These constants and other crystalline electrostatic potentials used in this paper were calculated by Ralph Guertin at the National Bureau of Standards.

¹⁰ F. J. Morin, Bell System Tech. J. **37**, 1047 (1958).

¹¹ Bleaney, Proc. Phys. Soc. (London) **A63**, 407 (1950).

¹² H. A. Weakliem and D. S. McClure, J. Appl. Phys. Suppl. **33**, 347 (1962).

¹³ L. B. Bouckaert, R. Smoluchowski, and E. Wigner, Phys. Rev. **50**, 65 (1936).

¹⁴ E. P. Wigner, *Group Theory and Its Applications to the Quantum Mechanics of Atomic Spectra* (Academic Press, Inc., New York, 1959), pp. 115-116.

TABLE I. Symmetrized Ti-3*d* orbitals and O-2*p* orbitals for cubic strontium titanate. Letters represent normalized atomic orbitals. Symmetry classification is according to the notation of BSW (Ref. 13); the prefixed number gives the dimension of the irreducible representation.

Representation	<i>d</i> orbitals	<i>p</i> orbitals	Representation	<i>d</i> orbitals	<i>p</i> orbitals
2 Γ ₁₂	(3 <i>z</i> ² - <i>r</i> ²), (<i>x</i> ² - <i>y</i> ²)		1 Σ ₃	(<i>xz</i>) + (<i>yz</i>)	(<i>z, z, 0</i>)
3 Γ _{25'}	(<i>xy</i>), (<i>yz</i>), (<i>zx</i>)		1 Σ ₃		(0, 0, <i>z</i>)
3 Γ ₁₅		(<i>x, 0, 0</i>), (0, <i>y, 0</i>), (0, 0, <i>z</i>)	1 Σ ₄	(<i>x</i> ² - <i>y</i> ²)	(<i>x</i> , - <i>y</i> , 0)
3 Γ ₁₅		(0, <i>x, x</i>), (<i>y, 0, y</i>), (<i>z, z, 0</i>)	1 Σ ₄		(<i>y</i> , - <i>x</i> , 0)
3 Γ ₂₅		(<i>z</i> , - <i>z</i> , 0), (0, <i>x</i> , - <i>x</i>), (- <i>y</i> , 0, <i>y</i>)	1 Σ ₄		[0, 0, (<i>x</i> - <i>y</i>)/√2]
1 X ₁	(3 <i>y</i> ² - <i>r</i> ²)	(0, <i>y, 0</i>)	1 A ₁	(<i>xy</i>) + (<i>yz</i>) + (<i>zx</i>)	(<i>x, y, z</i>)
1 X ₂	(<i>z</i> ² - <i>x</i> ²)		1 A ₁		(<i>z</i> + <i>y</i> , <i>x</i> + <i>z</i> , <i>x</i> + <i>y</i>)
1 X ₃	(<i>xz</i>)		1 A ₂		(<i>z</i> - <i>y</i> , <i>x</i> - <i>z</i> , <i>x</i> - <i>y</i>)
2 X ₅	(<i>xy</i>), (<i>yz</i>)	(0, <i>x, 0</i>), (0, <i>z, 0</i>)	2 A ₃	(<i>x</i> ² + ω ² <i>y</i> ² + ω ² <i>z</i> ²), (c.c.)	(<i>x, ω</i> ² <i>y, ωz</i>), (c.c.)
1 X _{3'}		(<i>y</i> , 0, - <i>y</i>)	2 A ₃	(<i>yz</i> + ω ² <i>zx</i> + ω ² <i>xy</i>), (c.c.)	(<i>y, ω</i> ² <i>z, ωx</i>), (c.c.)
1 X _{4'}		(<i>y, 0, y</i>)	2 A ₃	[ω = exp(2π <i>i</i> /3)]	(<i>z, ω</i> ² <i>x, ωy</i>), (c.c.)
2 X _{5'}		(<i>x, 0, 0</i>), (0, 0, <i>z</i>)	1 Z ₁	(<i>x</i> ² - <i>y</i> ²)	(<i>x, 0, 0</i>)
2 X _{5'}		(0, 0, <i>x</i>), (<i>z, 0, 0</i>)	1 Z ₁	(3 <i>z</i> ² - <i>r</i> ²)	(0, <i>y, 0</i>)
1 M ₁	(3 <i>z</i> ² - <i>r</i> ²)	(<i>x, y, 0</i>)	1 Z ₁		(0, 0, <i>x</i>)
1 M ₂	(<i>x</i> ² - <i>y</i> ²)	(<i>x</i> , - <i>y</i> , 0)	1 Z ₂	(<i>yz</i>)	(0, <i>z, 0</i>)
1 M ₃	(<i>xy</i>)	(<i>y, x, 0</i>)	1 Z ₃	(<i>xy</i>)	(0, 0, <i>y</i>)
1 M ₄		(<i>y</i> , - <i>x</i> , 0)	1 Z ₃		(0, <i>x, 0</i>)
2 M ₅	(<i>yz</i>), (<i>zx</i>)	(0, <i>z, 0</i>), (<i>z, 0, 0</i>)	1 Z ₃		(<i>y, 0, 0</i>)
1 M _{4'}		(0, 0, <i>z</i>)	1 Z ₄	(<i>xz</i>)	(<i>z, 0, 0</i>)
2 M _{5'}		(0, 0, <i>x</i>), (0, 0, <i>y</i>)	1 Z ₄		(0, 0, <i>z</i>)
1 R ₁		(<i>x, y, z</i>)	1 S ₁	(<i>xz</i>)	(<i>x, 0, z</i>)
2 R ₁₂	(<i>x</i> ² - <i>y</i> ²), (3 <i>z</i> ² - <i>r</i> ²)	(<i>x</i> , - <i>y</i> , 0), (- <i>x</i> , - <i>y</i> , 2 <i>z</i>)	1 S ₁	(3 <i>y</i> ² - <i>r</i> ²)	(<i>z, 0, x</i>)
3 R _{25'}	(<i>yz</i>), (<i>zx</i>), (<i>xy</i>)	(0, <i>z, y</i>), (<i>z, 0, x</i>), (<i>y, x, 0</i>)	1 S ₁		(0, <i>y, 0</i>)
3 R _{15'}		(0, <i>z</i> , - <i>y</i>), (- <i>z</i> , 0, <i>x</i>), (- <i>y</i> , <i>x</i> , 0)	1 S ₂	(<i>xy</i>) - (<i>zy</i>)	(<i>y</i> , 0, - <i>y</i>)
1 Δ ₁	(3 <i>y</i> ² - <i>r</i> ²)	(0, <i>y, 0</i>)	1 S ₂		(0, <i>x</i> - <i>z</i> , 0)
1 Δ ₁		(<i>y, 0, y</i>)	1 S ₃	(<i>xy</i>) + (<i>zy</i>)	(<i>y, 0, y</i>)
1 Δ ₂	(<i>z</i> ² - <i>x</i> ²)	(<i>y</i> , 0, - <i>y</i>)	1 S ₃		(0, <i>x</i> + <i>z</i> , 0)
1 Δ _{2'}	(<i>xz</i>)		1 S ₄	(<i>x</i> ² - <i>z</i> ²)	(<i>x</i> , 0, - <i>z</i>)
2 Δ ₅	(<i>xy</i>), (<i>yz</i>)	(<i>x, 0, 0</i>), (0, 0, <i>z</i>)	1 S ₄		(<i>z</i> , 0, - <i>x</i>)
2 Δ ₅		(0, <i>x, 0</i>), (0, <i>z, 0</i>)	1 T ₁	(3 <i>z</i> ² - <i>r</i> ²)	(0, 0, <i>z</i>)
2 Δ ₅		(0, 0, <i>x</i>), (<i>z, 0, 0</i>)	1 T ₁		(<i>x, y, 0</i>)
1 Σ ₁	(<i>xy</i>)	(<i>x, y, 0</i>)	1 T ₂	(<i>x</i> ² - <i>y</i> ²)	(<i>x</i> , - <i>y</i> , 0)
1 Σ ₁	(3 <i>z</i> ² - <i>r</i> ²)	(<i>y, x, 0</i>)	1 T _{1'}		(<i>y</i> , - <i>x</i> , 0)
1 Σ ₁		[0, 0, (<i>x</i> + <i>y</i>)/√2]	1 T _{2'}	(<i>xy</i>)	(<i>y, x, 0</i>)
1 Σ ₂	(<i>xz</i>) - (<i>yz</i>)	(<i>z</i> , - <i>z</i> , 0)	2 T ₅	(<i>xz</i>), (<i>yz</i>)	(<i>z, 0, 0</i>), (0, <i>z, 0</i>)
			2 T ₅		(0, 0, <i>x</i>), (0, 0, <i>y</i>)

1. Diagonal Elements—Ti

A typical diagonal element of the energy with respect to an *xy*-type Bloch sum, for example, is given by

$$\langle xy | \mathcal{H} | xy \rangle = \int \phi_{xy}(\mathbf{r}) \left[-(\hbar^2/2m)\nabla^2 + V_{\text{Ti}}(\mathbf{r}) + \sum_i V_{\text{Ti}}(\mathbf{r} - \mathbf{R}_i) + \sum V_0 + \sum V_{\text{Sr}} \right] \phi_{xy}(\mathbf{r}) d\mathbf{r}, \quad (3)$$

where the *V*'s represent the potentials of the respective ions. In Eq. (3) we have neglected Ti-Ti overlap. We estimate this integral by using free-ion wave functions and a point-ion model for the potentials of all ions except the central Ti of the integral. We expand the point-ion potential, using the ionic charges determined in Sec. II, to fourth order around the central Ti. Then the successive terms represent the ionization potential of Ti³⁺, the Madelung potential at the Ti site, and the shift of the *d* state in the cubic crystalline electrostatic

field. The *d* splitting by the crystalline field is estimated by using Watson's Ti³⁺ Hartree-Fock wave function.¹⁵

TABLE II. Numerical parameters (in eV) used in the tight binding calculation for SrTiO₃.

Ionization plus Madelung energy	Ti - 6.8
	O - 10.5
Electrostatic splitting of <i>d</i> orbitals ^a	0.62
Electrostatic splitting of <i>p</i> orbitals ^b	0.48
Overlap integral (<i>pdσ</i>)	2.1
Overlap integral (<i>pdπ</i>) ≈ 0.4(<i>pdσ</i>) ^c	0.84
Overlap integral (<i>pπσ</i>)	- 0.16
Overlap integral (<i>ppπ</i>) ^d	0.062

^a Determined on the point-ion approximation with the Watson Ti³⁺ wave function.

^b Determined on the point-ion approximation with the Watson O²⁻ wave function.

^c Estimated by the method of Wolfsberg and Helmholz (gives agreement with experimental 10 *Dq* in molecular complexes).

^d Taken from Switendick's NiO calculation.

¹⁵ R. E. Watson, Technical Report No. 12, June 15, 1959, Solid State and Molecular Theory Group, MIT, Cambridge, Massachusetts (unpublished).

Thus the diagonal element reproduces the ionic estimate but also includes the crystal field splitting.

Our justification for the use of the point-ion approximation and neglect of the neighboring ion's electronic charge cloud is derived from the Phillips,¹⁶ Cohen-Heine¹⁷ "cancellation theorem." In the present context, the theorem states that the effect of orthogonalizing the Ti-3*d* orbital to the O-2*p* orbital is compensated by the finite extent of the charge density of the oxygen ion, and thus that the point-ion approximation is applicable. This approximation has been tested by Sugano and Shulman⁷ and found to be valid to within 20% in the perovskite structured KNiF₃.

2. Diagonal Elements—O

These elements have been considered with the inclusion of nearest neighbor O-O overlap terms. In a way similar to the case of Ti, the diagonal element is approximated by the ionization energy, the Madelung energy, a crystal field splitting, and now O-O overlap terms. The crystal field splitting of the 2*p* states occurs because the oxygen resides at a site of tetragonal *D*_{4*h*} (4/*mmm*) point symmetry, and experiences an axial field. For the ionization energy of O²⁻ we use -9 eV, the negative affinity deduced from the Born-Haber cycle and O⁻ ionization potential by Morin.¹⁰ The Watson O²⁻ 2*p* wave function was used to estimate the crystal field splitting, which we denote by $\frac{2}{3} \Delta$. The *p* state oriented parallel to the axial field is shifted twice that of those oriented transverse to the axial field. Finally the value of the overlap integrals⁴ (*pp* σ) and (*pp* π) were taken from the work of Switendick⁵ on NiO, in which the O-O distances are approximately the same as in SrTiO₃.

3. Off-diagonal Elements—Ti-O

These elements depend on the (*pd* σ) and (*pd* π) overlap integrals. We "borrow" these from two independent sources. First, we note that in almost all published work (*pd* π) \approx 0.4 (*pd* σ), and that energies are very insensitive to (*pd* π). We may estimate (*pd* σ) from the empirical recipe of Wolfsberg and Helmholz^{18,19} which states that the energy overlap integral is roughly equal to the wave function overlap integral multiplied by the sum of the diagonal energies of the two orbitals. This was performed with the Watson Ti³⁺ and O²⁻ functions.²⁰ An alternative estimate is obtained by choosing the value of (*pd* σ), with (*pd* π) \approx 0.4 (*pd* σ), which will give the correct 10 *Dq* splitting of 20 000 cm⁻¹ for Ti with octahedral coordination of neighboring oxygen

ions, as in Ti-alum or Ti³⁺ in corundum. We attribute the 10 *Dq* splitting primarily to the (*pd* σ) two-center overlap, and neglect the smaller effect of trigonal distortion and three-center contributions. The required (*pd* σ) agrees exactly with the estimate obtained by the Wolfsberg-Helmholz method. It is interesting to observe that a simple calculation with the Watson wave function for Ti³⁺ indicates that the electrostatic splitting of the *d* states accounts for only 20% of the full 20 000 cm⁻¹, and that the remainder must come from a degree of covalency which leads to an ionic charge for the oxygen of $\approx -1.7 e$.

IV. RESULTS AND DISCUSSION

The results of *E* versus *k* are plotted in Fig. 3. Some of the most significant features are now outlined.

The over-all picture of the conduction bands is that of 3*d* bands spread out by a large (*pd* σ) interaction, with smaller splittings by cubic crystalline fields and (*pd* π) interactions. The latter two are approximately equal in magnitude. At *k*=0, the *p* and *d* orbitals do not mix and the splitting is purely from the crystal field. At the edge of the zone the effect of (*pd* σ) is to produce the major contribution to the 4-eV bandwidth.

The valence bands are split at *k*=0 by axial crystalline fields and (*pp* σ) and (*pp* π) interactions, of the same relative magnitudes. Away from the origin the (*pd* σ) and (*pd* π) interactions are operative, the (*pd* σ) giving the largest contribution to the bandwidth of ~ 4 eV.

The lowest conduction band is flat along the cubic axes, i.e., the longitudinal mass is infinite, the transverse mass $m_1 \approx 1m_0$. In all other directions of *k* space the energy rises. Inclusion of Ti-Ti overlap would cause this lowest conduction band to curve downward along the cubic axes, depressing the band at the edge of the BZ by about 0.02-0.05 eV, corresponding to a longitudinal mass $\approx 20-50 m_0$. Spin-orbit interaction would further split $\Gamma_{25'}$, by the order of ≈ 0.03 eV, suggesting a probability of observing multiple-band conduction at 77°K and higher.

The prediction of <100> ellipsoids for the lowest conduction band is almost completely a consequence of symmetry, i.e., it follows from the fact that the Δ_2' titanium 3*d* orbital does not mix with any oxygen orbitals, together with reasonable assumptions of the splitting of *d* states in cubic environment.

Strong support for the model of <100> conduction band ellipsoids is found in preliminary measurements of magnetoresistance by Becker and Frederikse.²¹ Values of the ratio of transverse to longitudinal magnetoresistance, with current in the [100] direction, were observed to be as high as 10.

There is some experimental verification of the valence bandwidth in the soft x-ray emission spectra of SrTiO₃, BaTiO₃, and TiO₂. The breadths of the TiK _{β_5} spectra

¹⁶ J. C. Phillips, Phys. Chem. Solids **11**, 226 (1959).

¹⁷ M. H. Cohen and V. Heine, Phys. Rev. **122**, 1821 (1961).

¹⁸ M. Wolfsberg and L. Helmholz, J. Chem. Phys. **20**, 837 (1952).

¹⁹ C. J. Ballhausen, *Introduction to Ligand Field Theory* (McGraw-Hill Book Company, Inc., New York, 1962), pp. 161-162.

²⁰ R. E. Watson, Phys. Rev. **111**, 1108 (1958).

²¹ H. P. R. Frederikse and J. H. Becker (to be published).

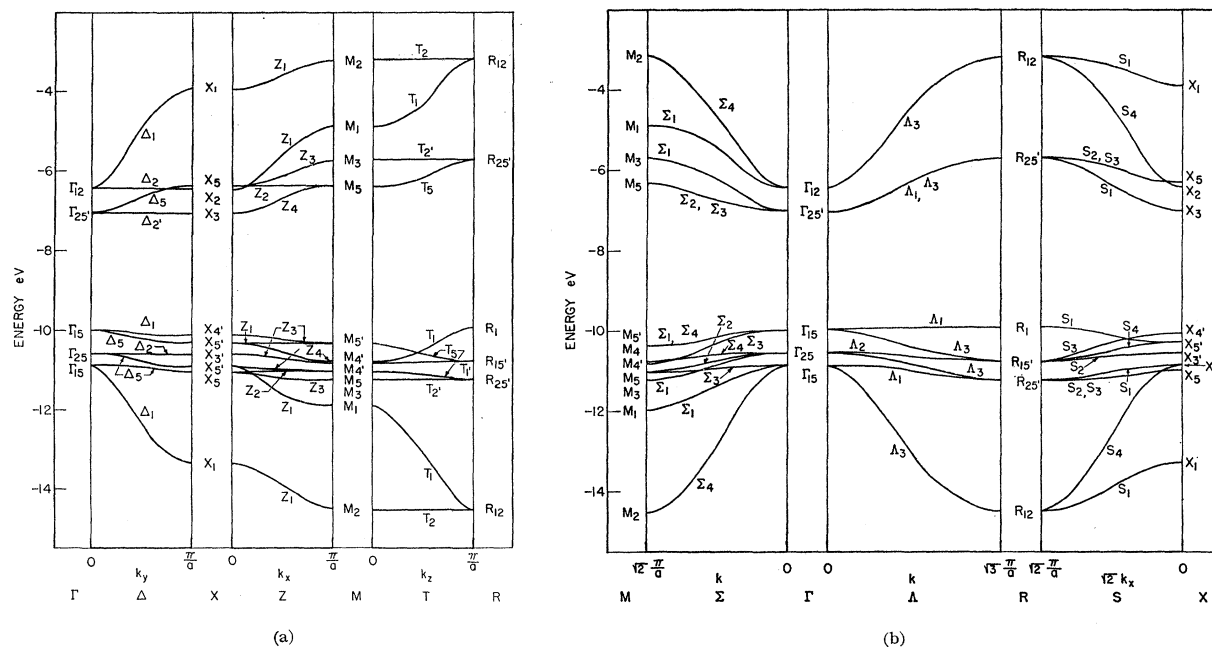


FIG. 3. (a) and (b) Plot of energy versus wave vector for all lines of symmetry of the Brillouin zone.

observed were 3.55, 2.86, and 3.63 eV,²² respectively. It is expected that the (*pd* σ) interactions will be comparable in these substances.

Reflectivity measurements on rutile²³ show considerable structure up to 13 eV, which is comparable to the over-all breadth of conduction and valence bands.

From Hall effect and Seebeck coefficient measurements it is possible to determine a density of states effective mass. Frederikse *et al.*² find that for *n*-type reduced SrTiO₃, m^* varies from $\sim 16m_0$ at 300°K to $\sim 6m_0$ at 78°K. This is in reasonable agreement with values of 6–12 m_0 obtained from this calculation, the variation coming from estimates of the Ti-Ti overlap. Inclusion of polaron effects would certainly increase the calculated effective masses.

A calculation similar to this has been considered for

²² M. A. Blokhin and A. T. Shuvaev, Bull. Acad. Sci. USSR, Physical Series 26, 429 (1962), Columbia Technical Translations.

²³ M. Cardona (private communication).

rutile (TiO₂). The results are complicated by the orthorhombic environment of the Ti ion which splits the $\Gamma_{25'}$ *d* states by the order of several hundredths of an eV, which is of the same order of magnitude as the splitting by spin-orbit interaction. It is very likely that the results for the conduction band edge will be similar to those of SrTiO₃, i.e., ellipsoids with heavy longitudinal masses and the presence of higher conduction bands several hundredths of an eV higher, as determined experimentally by Becker.¹

ACKNOWLEDGMENTS

The authors are grateful to Dr. H. P. R. Frederikse for suggesting this study on SrTiO₃, to Ralph F. Guertin for calculations of crystalline electric fields, and to Philip J. Walsh for computer programming. Numerous colleagues at the National Bureau of Standards contributed through helpful discussion.